Table I. Photoproduct Percentages (Corrected for Detector Response and Extrapolated to 0% Conversion) as a Function of Reaction Medium and Temperature[a-c]

diketone	medium	temp, °C	% 2	% 3	% 4
1a	crystal	20	89	10	1
	crystal	30	47	16	37
	crystal	40	17	20	63
	soln	20	22 (0.019)	35 (0.031)	43 (0.054)
	soln	40	19	30	51
1b	crystal	20	3	84	13
	soln	20	17 (0.015)[d]	42 (0.038)	41 (0.045)
1c	crystal	20	4	91	5
	soln	20	10 (0.009)[d]	34 (0.032)	56 (0.037)

[a] Quantum yields in parentheses. [b] The Pyrex-filtered output of a 450-W Hanovia medium-pressure mercury lamp was the light source in both the solid-state and the solution-phase (hexane) photolyses. At this wavelength, only the n,π^* absorption band (λ_{max} ca. 280 nm, ϵ = 60 for all three diketones in acetonitrile) was excited. The solid-state UV spectra were qualitatively similar to those measured in solution. [c] The range of conversion levels varied between 2% and 15%; over this range, the extrapolation to 0% conversion was linear. [d] Partial overlapping of peaks on GC makes these quantum yields and product percentages somewhat less precise.

Table I gives the product percentages resulting from Pyrex-filtered irradiation of diketones **1a-c** under various experimental conditions. We draw attention to three main trends that are evident in the data: (1) the proportion of type II cyclization (photoproducts **2** and **3**) is greater in the solid state than in solution; (2) the stereoselectivity of cyclobutanol formation increases in the solid state compared to solution; particularly striking is the *reversal* in cyclobutanol stereoselectivity observed in the case of diketone **1a**; and (3) for diketone **1a**, the solid-state photoproduct distribution (but not the solution-phase distribution) depends dramatically on the photolysis temperature.

The first two observations are explicable in terms of the well-established idea that solid-state chemical reactions tend to be topochemically controlled[10] and, in the case of unimolecular processes, conformation-specific.[11] Diketones **1a** and **1c** have very different conformations (Figure 1); the abstracting oxygen atoms and the *nonabstracted* γ-hydrogen atoms (which end up as the ring junction methine protons) are syn to one another in **1a** and anti in **1c** (and **1b**). Thus the process of hydrogen abstraction and cyclobutanol formation involving retention of configuration at both the carbonyl carbon and the γ-carbon leads, in a natural and topochemical fashion, to the cis-fused cyclobutanol **2a** from **1a** and to the trans-fused cyclobutanols **3c** and **3b** from **1c** and **1b**, respectively. This argument is valid regardless of which of the accessible γ-hydrogen atoms is abstracted in each case. Inspection of the packing diagrams does not reveal any obvious *inter*molecular contacts that might account for the stereoselectivities observed. In solution, reaction from other diketone conformers as well as possible conformational isomerization of the intermediate 1,4-biradicals leads to a greater degree of type II elimination plus a preference for formation of the presumably less strained cyclobutanols **3a-c** in each case.[12]

The dramatic change in the solid-state photoproduct percentages for diketone **1a** between 20 and 40 °C (Table I) deserves comment. This is due to a solid-solid phase transition that occurs in this temperature range, well below the melting point of 86 °C. This phase transition was first noted by Alvik, Borgen, and Dale,[9] who reported it as occurring at 28 °C; our own highly reproducible differential scanning calorimetry measurements indicate a transition temperature of 34 °C.[13] The nature of the high-temperature solid phase is under active investigation at the present time. From the photochemical results, however, it appears that this phase mimics the situation in solution to a considerable degree.

Acknowledgement is made to the donors of the Petroleum Research Fund, administered by the American Chemical Society, for partial support of this research. Financial support by the Natural Sciences and Engineering Research Council of Canada is also gratefully acknowledged.

Registry No. 1a, 31067-25-1; **1b**, 13747-10-9; **1c**, 38300-52-6; **2a**, 125735-63-9; **2b**, 125735-65-1; **2c**, 125735-67-3; **3a**, 125826-55-3; **3b**, 125826-56-4; **3c**, 125826-57-5; **4a**, 125735-64-0; **4b**, 125735-66-2; **4c**, 125735-68-4.

(10) (a) Schmidt, G. M. J. *Pure Appl. Chem.* **1971**, *27*, 647. (b) Cohen, M. D. *Angew. Chem., Int. Ed. Engl.* **1975**, *14*, 386.

(11) Ariel, S.; Evans, S.; Hwang, C.; Jay, J.; Scheffer, J. R.; Trotter, J.; Wong, Y.-F. *Tetrahedron Lett.* **1985**, *26*, 965.

(12) Quenching studies indicate that diketones **1a-c**, like other aliphatic ketones, undergo the Norrish type II reaction from both singlet and triplet excited states. Since it is well established that triplets generally cyclize to a greater extent than singlets,[3] part of the increased degree of cyclization observed in the solid state for compounds **1a-c** may stem from enhanced intersystem crossing in this medium relative to solution.

(13) An analogous phase transition was observed at 86 °C for diketone **1b** (mp 96 °C), and a similar (but less dramatic) variation in the solid-state photoproduct ratios above and below the transition point was found. No phase transition was detectable in the case of diketone **1c**, however.

Kinetic Effect of a Syn-Oriented Carboxylate on a Proximate Imidazole in Catalysis: A Model for the Histidine-Aspartate Couple in Enzymes

Katherine D. Cramer and Steven C. Zimmerman*

Department of Chemistry, University of Illinois Urbana, Illinois 61801

Received January 18, 1990

The catalytic dyad of histidine and aspartate (glutamate), known as the His-Asp couple (**1**), has been found in the active site of zinc-containing enzymes,[1a] glutathione reductase,[1b] phospholipase A_2,[1c] the serine proteases,[1d,e] malate and lactate dehydrogenase,[1f] and DNAse I,[1g] and possibly in ribonuclease T_1.[1h,i] In all but the zinc enzymes, the histidine residue has been proposed to act as a general acid/base[1] or, less frequently, as a nucleophile.[2] If convergent evolution has led to the presence of the His-Asp couple in these many enzymes, then the carboxylate must play an important structural and/or catalytic role.

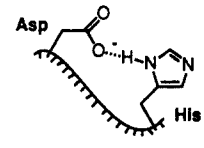

1

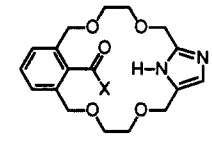

2: X = O⁻
3: X = NH_2

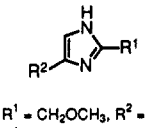

4: R^1 = CH_2OCH_3, R^2 = CH_3
5: R^1 = $CH_2CH_2OCH_3$, R^2 = CH_3
6: R^1 = CH_2CH_3, R^2 = CH_3

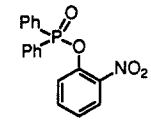

7

The nature of this role is not known, but has been the subject of intense debate, particularly in the case of the serine proteases.[3]

(1) (a) Christianson, D. W.; Alexander, R. S. *J. Am. Chem. Soc.* **1989**, *111*, 6412-6419. (b) Karplus, P. A.; Pai, E. F.; Schultz, G. E. *Eur. J. Biochem.* **1989**, *178*, 693-703. (c) Dijkstra, B. W.; Drenth, J.; Kalk, K. H. *Nature (London)* **1981**, *289*, 604-606. (d) Blow, D. M.; Birktoft, J. J.; Hartley, B. S. *Nature (London)* **1969**, *221*, 337-340. (e) Kraut, J. *Annu. Rev. Biochem.* **1977**, *46*, 331-358. (f) Birktoft, J. J.; Banaszak, L. J. *J. Biol. Chem.* **1983**, *258*, 472-482. (g) Suck, D.; Oefner, C. *Nature (London)* **1988**, *332*, 464-468. (h) Nishikawa, S.; Morioka, H.; Kim, H. J.; Fuchimura, K.; Tanaka, T.; Uesugi, S.; Hakoshima, T.; Tomita, K.; Ohtsuka, E.; Ikehara, M. *Biochemistry* **1987**, *26*, 8620-8624. (i) See, however: Mossakowska, D. E.; Nyberg, K.; Fersht, A. R. *Biochemistry* **1989**, *28*, 3843-3850.

(2) Hubbard, C. D.; Kirsch, J. F. *Biochemistry* **1972**, *11*, 2483-2493. Quinn, D. M.; Elrod, J. P.; Ardis, R.; Friesen, P.; Schowen, R. L. *J. Am. Chem. Soc.* **1980**, *102*, 5358-5365.

0002-7863/90/1512-3680$02.50/0

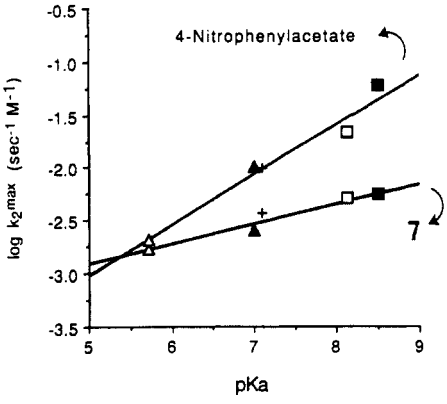

Figure 1. Brønsted plots for the reaction of imidazole **2** (+), **3** (△), **4** (▲), **5** (□), and **6** (■) with 4-nitrophenylacetate (β = 0.49) and **7** (β = 0.18). Data from Table I.

These enzymes hydrolyze specific substrates with "two proton transfer" catalysis, supporting a general base mechanism for Asp-102.[4] However, titration of the enzymes, either alone[5] or inhibited with transition-state analogues,[6] shows His-57 to be the more basic residue, arguing against proton transfer to Asp-102. Replacement of Asp-102 by asparagine (D102N)[7a] or alanine (D102A)[7b,c] using site-directed mutagenesis results in mutant enzymes with dramatic 10^4-fold decreases in turnover number. Apparently, this factor of 10^4 does not represent the contribution of Asp-102 alone since its replacement in trypsin causes His-57 to shift from the active N-3(H) to the inactive N-1(H) tautomer.[8] In this regard, models of the His-Asp couple may provide the best opportunity to examine the role of the carboxylate without altering the role of the imidazole. The proximate carboxylate in reported models provides only a minimal rate enhancement in acyl-transfer reactions in aqueous media.[9,10] However, Gandour has noted that these models contain anti-oriented carboxylates, whereas the enzymes feature a syn disposition.[11] A *syn*-carboxylate is proposed to be 10^3–10^4 times more basic than an *anti*-carboxylate.[11]

We have investigated the *catalytic* properties of **2**, our previously reported syn-oriented model of the His-Asp couple.[12,13] Comparison with amide **3** and 2,4(5)-disubstituted imidazoles **4–6** has allowed the catalytic role of the carboxylate to be determined.[14] Since the natural substrates are too unreactive for model studies, and since enzymes containing the His-Asp couple catalyze several different processes, the exact reaction examined is less important than its mechanism. Thus, we have examined two reactions, one proceeding by a nucleophilic and the other by a general base mechanism. Acyl transfer to imidazole (nucleophilic catalysis) was examined with 4-nitrophenylacetate as substrate.[15] As seen in Figure 1, a linear Brønsted plot can be constructed with compounds **2–6**. His-Asp model **2** fits well on the plot. Indeed **2** and **4**, which have nearly identical pK_a values, react with 4-nitrophenylacetate at the same rate (Table I) even though the latter compound lacks the additional catalytic group. This argues against a general base role for the carboxylate. Further support for this conclusion comes from the identical solvent isotope effect for **2** (k_{H2O}/k_{D2O} = 1.25 ± 0.08) and **6** (k_{H2O}/k_{D2O} = 1.2 ± 0.1), both of which indicate a predominantly nucleophilic mechanism.[16]

In order to determine the role played by the *syn*-carboxylate of **2** in a general base catalyzed process, the hydrolysis of 2-nitrophenyl diphenylphosphinate (**7**) was investigated. Aryl diphenylphosphinates have been shown to undergo general base catalyzed hydrolysis by imidazole, and they are substrates for chymotrypsin.[17] As seen in Figure 1, **2** fits on a Brønsted plot with **3–6**, all points deviating by less than 21% in their k_2^{max} values. The solvent isotope effect for **2** (k_{H2O}/k_{D2O} = 2.08 ± 0.03) is within experimental error of that for **6** (k_{H2O}/k_{D2O} = 1.9 ± 0.2) and in the range expected for general base catalyzed hydrolysis with proton transfer from water to the imidazole.[16,17] As in nucleophilic catalysis, the *syn*-carboxylate does not enhance the reactivity of the imidazole by acting as a base.

With one exception, enzymes containing the His-Asp couple have syn-oriented carboxylates.[12] While a syn-oriented carboxylate may provide a more basic lone pair and/or greater electrostatic stabilization than an *anti*-carboxylate, the corresponding increase in basicity of a proximate imidazole is small.[12,13] The results reported herein show that the *catalytic* benefit of a *syn*-carboxylate is minimal and limited to this small pK_a increase, consistent with the Brønsted catalysis law. Thus, **7** is hydrolyzed by His-Asp model **2** only 2 times faster than it is by amide **3**. While the amide could donate a hydrogen bond to the imidazole in **3**, producing an unproductive imidazole tautomer, it is not constrained to do so as it is in D102N trypsin.[8] In this sense the model and mutagenesis studies are complementary. The former show that the

Table I. Equilibrium pK_a Values of Imidazolium Compounds **2–6** and Second-Order Rate Constants for Their Reaction with 4-Nitrophenylacetate and 2-Nitrophenyl Diphenylphosphinate[a]

imidazole	pK_a	solvent	4-nitrophenylacetate: k_2^{max} × 10^3 M^{-1} s^{-1}	2-nitrophenyl diphenylphosphinate: k_2^{max} × 10^3 M^{-1} s^{-1}
2	7.05 ± 0.05	H_2O	10.0 ± 0.4	3.74 ± 0.04
2	7.50 ± 0.08[b]	D_2O	8.0 ± 0.4	1.80 ± 0.02
3	5.72 ± 0.02	H_2O	2.0 ± 0.1	1.79 ± 0.08
3	6.15 ± 0.06[b]	D_2O		
4	7.03 ± 0.01	H_2O	10.2 ± 0.6	2.6 ± 0.2
5	8.13 ± 0.02		21.4 ± 0.1	5.0 ± 0.3
6	8.50 ± 0.02		60.0 ± 1.0	5.6 ± 0.4
6	8.62 ± 0.04	D_2O	52.0 ± 6.0	2.9 ± 0.1

[a] pK_a values were determined by potentiometric titration at 25 °C, μ = 0.5 (KCl). Second-order rate constants (k_2) at 25 °C, μ = 0.5 (KCl), were determined from plots of k_{obsd} against imidazole concentration. Maximal second-order rate constants were calculated from $k_2 = k_2^{max}K_a/([H^+] + K_a)$. [b] Reference 12.

(3) Polgár, L.; Halász, P. *Biochem. J.* **1982**, *207*, 1–10. Schowen, R. L. In *Principles of Enzyme Activity*; Liebman, J. F., Greenberg, A., Eds.; VCH: New York; 1988, Vol. 9.

(4) Venkatasubban, K. S.; Schowen, R. L. *CRC Crit. Rev. Biochem.* **1984**, *17*, 1–44. Stein, R. L.; Strimpler, A. M. *J. Am. Chem. Soc.* **1987**, *109*, 4387–4390. See, however: Scholten, J. D.; Hogg, J. L.; Raushel, F. M. *J. Am. Chem. Soc.* **1988**, *110*, 8246–8247.

(5) (a) Bachovchin, W. W.; Roberts, J. D. *J. Am. Chem. Soc.* **1978**, *100*, 8041–8047. (b) Markley, J. L.; Ibanez, I. B. *Biochemistry* **1978**, *17*, 4627–4640.

(6) Kossiakoff, A. A.; Spencer, S. A. *Nature (London)* **1980**, *288*, 414–416. Kossiakoff, A. A.; Spencer, S. A. *Biochemistry* **1981**, *20*, 6462–6474.

(7) (a) Craik, C. S.; Roczniak, S.; Largman, C.; Rutter, W. J. *Science (Washington, D.C)* **1987**, *237*, 909–913. (b) Carter, P.; Wells, J. A. *Nature (London)* **1988**, *332*, 564–568. (c) See also: Clarke, A. R.; Wilks, H. M.; Barstow, D. A.; Atkinson, T.; Chia, W. N.; Holbrook, J. J. *Biochemistry* **1988**, *27*, 1617–1622.

(8) Sprang, S.; Standing, T.; Fletterick, R. J.; Stroud, R. M.; Finer-Moore, J.; Xuong, N.-H.; Hamlin, R.; Rutter, W. J.; Craik, C. S. *Science (Washington, D.C.)* **1987**, *237*, 905–909.

(9) (a) Rogers, G. A.; Bruice, T. C. *J. Am. Chem. Soc.* **1974**, *96*, 2473–2481. (b) Komiyama, M.; Bender, M. L. *Bioorg. Chem.* **1977**, *6*, 13–20. (c) Skorey, K. I.; Somayaji, V.; Brown, R. S. *J. Am. Chem. Soc.* **1989**, *111*, 1445–1452.

(10) An interesting preliminary report of a larger rate enhancement has appeared for an *anti*-imidazole–carboxylate in aqueous–organic solvent, but its mechanism has not been determined: Mallick, I. M.; D'Souza, V. T.; Yamaguchi, M.; Lee, J.; Chalabi, P.; Gadwood, R. C.; Bender, M. L. *J. Am. Chem. Soc.* **1984**, *106*, 7252–7254.

(11) Gandour, R. D. *Bioorg. Chem.* **1981**, *10*, 169–176.

(12) (a) Zimmerman, S. C.; Cramer, K. D. *J. Am. Chem. Soc.* **1988**, *110*, 5906–5908. (b) For **1**, the pK' values, pK'_{COOH} = 3.8 and pK'_{Im} = 7.50, are higher, but of similar magnitude to those seen in chymotrypsin A_α (p$K'_{Asp-102}$ = 2.8 and pK'_{His-57} = 6.1) and α-lytic protease (p$K_{a_{Im}}$ = 7.0); see ref 5.

(13) For another syn model, see: Huff, J. B.; Askew, B.; Duff, R. J.; Rebek, J., Jr. *J. Am. Chem. Soc.* **1988**, *110*, 5908–5909. See also: Li, Y.; Houk, K. N. *J. Am. Chem. Soc.* **1989**, *111*, 4505–4507.

(14) All compounds used in this study had correct elemental analyses and had spectroscopic properties in accord with the assigned structure. Compounds **4** and **5** were prepared by a procedure analogous to that described in the following: Zimmerman, S. C.; Cramer, K. D.; Galan, A. A. *J. Org. Chem.* **1989**, *54*, 1256–1264.

(15) Bender, M. L. Turnquest, B. W. *J. Am. Chem. Soc.* **1957**, *79*, 1652–1655. Bruice, T. C.; Schmir, G. L. *J. Am. Chem. Soc.* **1957**, *79*, 1663–1667.

(16) Bender, M. L.; Bergeron, R. J.; Komiyama, M. *The Bioorganic Chemistry of Enzymatic Catalysis*; Wiley: New York, 1984; pp 91–96.

(17) Williams, A.; Naylor, R. A. *J. Chem. Soc. B* **1971**, 1967–1972. Douglas, K. T.; Williams, A. *J. Chem. Soc., Perkin Trans. 2* **1976**, 515–521.

carboxylate provides only a small direct catalytic advantage, while the latter reveal an essential, and predicted,[5a] role of Asp-102, providing the correct tautomeric form of His-57.

Acknowledgment. Funding from the National Institutes of Health (GM39782) and the National Science Foundation (CHE 58202) is gratefully acknowledged. S.C.Z. acknowledges a Dreyfus Teacher-Scholar Award, an Eli Lilly Granteeship, and an NSF Presidential Young Investigator Award.

Real-Time Measurements of Interfacial Charge Transfer Rates at Silicon/Liquid Junctions

Malcolm D. E. Forbes and Nathan S. Lewis*

Contribution No. 8097
Division of Chemistry and Chemical Engineering
California Institute of Technology
Pasadena, California 91125

Received January 8, 1990

The rates of interfacial charge transfer from photogenerated carriers in semiconductor electrodes to solution donors and acceptors are fundamentally important in the area of semiconductor electrochemistry.[1-3] However, to date there have been no real-time measurements of the charge-transfer rates between semiconductors and outer sphere redox couples. Previous steady-state current-voltage experiments have led to the suggestion that such rates might be extremely fast ($>10^{11}$ s^{-1}), because evidence has been obtained for interfacial charge transfer events competing with thermalization of the photoexcited carriers (i.e. "hot carrier injection processes").[4] Additionally, luminescence decay measurements on CdS surfaces in contact with strongly adsorbing, inner sphere redox reagents such as 1.0 M KOH/1.0 M S^{2-} have indicated high surface recombination velocities ($>10^5$ cm/s) and have yielded photoexcited carrier lifetimes of less than 100 ps.[5] In contrast, simple theoretical estimates of the interfacial charge transfer rate constants for outer sphere redox systems[1,2] can be used to predict carrier lifetimes between 10^{-6} and 10^{-3} s under common experimental conditions. To address these issues, we report herein the first real-time kinetic rate measurements from carriers in a semiconductor to outer sphere redox donors and acceptors in the liquid phase.

The carrier lifetime measurements in this work were obtained by microwave and radio-frequency (rf) conductivity techniques.[6,7] Previous studies on semiconductors (either in contact with air or with aqueous acids) have shown that, in proper experimental geometries, the intensity of the reflected microwave[6] (38.3-GHz, 180-mW source in our work) or rf[7] power (450 MHz, 1 W), P_{dark}, is proportional to the conductivity (σ) of the sample. Accordingly,

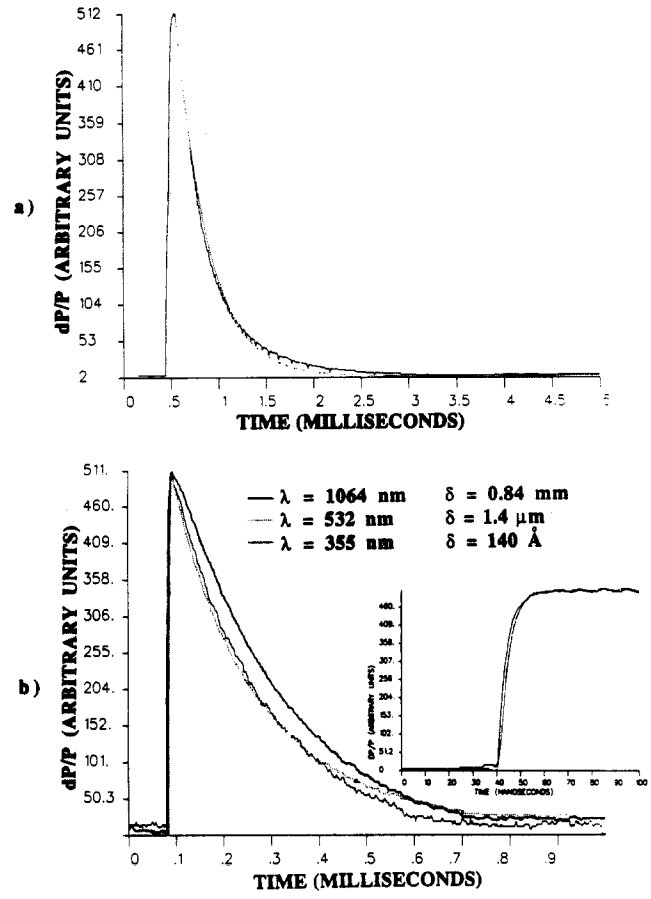

Figure 1. (a) Microwave conductivity decay (solid curve) under high injection (10^{15} injected carriers/cm^2 in a 190-μm-thick sample of n-Si) in contact with concentrated sulfuric acid. A simulation with a surface recombination velocity of 25 cm s^{-1} and a bulk lifetime of 2 ms is shown (dashed line) for comparison. Similar decay curves were obtained with a 450-MHz rf conductivity apparatus. (b) Microwave conductivity decays for the same material as in Figure 1a, but in contact with a methanol solution containing 0.34 M Me_2Fc, 5 mM Me_2Fc^+, and 0.10 M $LiClO_4$. Decays are displayed for three separate excitation wavelengths of penetration depth δ. The ratio of absorbed photons-cm^{-2}(Si) to maximum signal intensity is the same for all three curves. Absorbed photons per square centimeter (Si) were 2.2×10^{13} photons cm^{-2} at 1064 nm, 9.1×10^{12} photons cm^{-2} at 532 nm, and 1.7×10^{13} photons cm^{-2} at 355 nm. The light pulses were obtained from a Nd:YAG laser (Spectra-Physics Model DCR-1) with a 9-ns pulse width (fwhm). The inset shows the early time signals for all three wavelengths, and the rise time in these traces is preamplifier response limited.

upon creation of a nonequilibrium excess carrier concentration with a light pulse,

$$\Delta P/P_{dark} \propto \Delta\sigma = (\mu_n \Delta n + \mu_p \Delta p)q \qquad (1)$$

where μ_n and μ_p are the electron and hole mobilities, respectively, Δn and Δp are the excess electron and hole concentrations, q is the electronic charge, and ΔP is $P_{light} - P_{dark}$. Thus, if the mobilities are known, the time dependence of $\Delta P/P_{dark}$ allows measurement of the time dependence of the photoexcited carrier concentration in the semiconductor.[6,7] The advantages of this method are that it is contactless, has fast time resolution, allows collection of data from a single excitation pulse, and is feasible in a variety of electrolytes. High-injection conditions have been utilized in our work in order to minimize effects of the electric field in the semiconductor;[7-9] thus, only carrier diffusion to the surface of the sample must be considered as an alternative rate-limiting step.

Figure 1a shows the time dependence of the reflected microwave power for a 130 Ω cm resistivity (donor density = 3.4×10^{13} cm^{-3}),

(1) Gerischer, H. *Adv. Electrochem. Electrochem. Eng.* **1966**, *4*, 249.
(2) Morrison, S. R. *Electrochemistry of Semiconductor and Oxidized Metal Electrodes*; Plenum Press: New York, 1980.
(3) Finklea, H. O. *Semiconductor Electrodes*; Elsevier: Amsterdam, 1988.
(4) (a) Ross, R. T.; Nozik, A. J. *J. Appl. Phys.* **1982**, *53*, 3813. (b) Cooper, G.; Turner, J. A.; Parkinson, B. A.; Nozik, A. J. *J. Appl. Phys.* **1983**, *54*, 6463. (c) Kovel, C. A.; Segar, P. R. *J. Am. Chem. Soc.* **1989**, *111*, 2004.
(5) (a) Evenor, M.; Gottesfeld, S.; Harzion, Z.; Huppert, D.; Feldberg, S. W. *J. Phys. Chem.* **1984**, *88*, 6213. (b) Benjamin, D.; Huppert, D. *J. Phys. Chem.* **1988**, *92*, 4676.
(6) (a) Warman, J. M.; de Haas, M. P.; Wentinck, H. M. *Radiat. Phys. Chem.* **1989**, *34*, 581. (b) Kunst, M.; Werner, J. *J. Appl. Phys.* **1985**, *58*, 2236. (c) Tributsch, H.; Messer, B. *Chem. Phys. Lett.* **1987**, *142*, 546. (d) Warman, J. M.; de Haas, M. P.; Gratzel, M.; Infelta, P. P. *Nature* **1984**, *310*, 305. (e) Warman, J. M.; de Haas, M. P.; van Hovell tot Westerflier, S. W. F. M.; Binsma, J. J. M..; Kolar, Z. I. *J. Phys. Chem.* **1989**, *93*, 5895.
(7) (a) Yablonovitch, E.; Allara, D. L.; Chang, C. C.; Gmitter, T.; Bright, T. B. *Phys. Rev. Lett.* **1986**, *57*, 249. (b) Yablonovitch, E.; Swanson, R. M.; Eades, W. D.; Weinberger, B. R. *Appl. Phys. Lett.* **1986**, *48*, 245. (c) Yablonovitch, E.; Sandroff, C. J.; Bhat, R.; Gmitter, T. *Appl. Phys. Lett.* **1987**, *51*, 439. (d) Yablonovitch, E. Proceedings of the 173rd Meeting of the Electrochemical Society, Chicago, IL, 1988.
(8) Feldberg, S. M.; Evenor, M.; Huppert, D.; Gottesfeld, S. *J. Electroanal. Chem.* **1985**, *185*, 209.
(9) Many, A.; Goldstein, Y.; Grover, N. B. *Semiconductor Surfaces*; North-Holland: Amsterdam, 1965.

0002-7863/90/1512-3682$02.50/0